Performance Deviation of PV Water Pumping System under Different Ambient Factors

Sahar S. Kaddah [1], Khaled M. Abo-Al-Ez [2], EL-H. Abd-Raboh [1], Sara A. Diab [1]

[1]Department of Electrical Engineering, Faculty of Engineering, Mansoura University, Mansoura, Egypt
[2] Department of Electrical, Electronic, and Computer Engineering, Centre for Distributed Power and Electronics Systems (CDPES), Cape Peninsula University of Technology (CPUT), South Africa

***Abstract*— The performance deviation of a PV/Water pumping system is inevitable due to the serious effect caused by major ambient factors. Those factors are mainly the partial shading condition (PSC) of the PV array, the angle of incidence (AOI) of the solar beam, the air mass (AM), and the dust. This paper develops an aggregated irradiance model that incorporates the effects of all the major ambient factors. This model is developed by estimating the hourly global irradiance on the tilted surface, then dividing it into its main components. After that the effect of each ambient factor is modeled in association to a particular component of the global irradiance. This paper also implements an improved variable step size maximum power point tracking (MPPT) algorithm that is suitable for multiple maximum power points occurring during PSC. Thereafter, the modeling of a complete PV/water pumping system is built using MATLAB. The performance deviation is analyzed with sunshine hours for a given day and site, focusing on the water flow rate under separate and combined effect of the investigated ambient factors.**

List of symbols

PV	Photovoltaic
PVWPS	Photovoltaic water pumping system
PSC	Partial shading condition
MPPT	Maximum power point tracking
P&O	Perturbation and observation
AOI	Angle of incidence
AM	Air mass
AMa	Absolute air mass
D_{by}	Bypass diode
T	Ambient temperature
S_h	Shading ratio [%]
Ai	Amorphous PV type
Pi	Poly-crystalline PV type
PI	Proportional integral controller
DP	Displacement pump
CP	Centrifugal pump
$\bar{I}$	Hourly global irradiance on horizontal surface [W/m^2]
$\bar{I}_T$	Hourly global irradiance on inclined surfaces [W/m^2]
$\bar{I}_{BT}$	Hourly beam irradiance on inclined surface [W/m^2]
$\bar{I}_{DT}$	Hourly diffuse irradiance on inclined surface [W/m^2]
$\bar{I}_{RT}$	Hourly reflected irradiance on inclined surface [W/m^2]
$\bar{I}_{DT,iso}$	Isotropic component of hourly diffuse irradiance on inclined surface [W/m^2]
$\bar{I}_{DT,hz}$	Horizon component of hourly diffuse irradiance on inclined surface [W/m^2]
$\bar{I}_{DT,cs}$	Circumsolar component of hourly diffuse irradiance on inclined surface [W/m^2]
f_d	Fraction of diffuse irradiance used by module
P_{sh}	Power output at PSC [W]
$P_{No,sh}$	Power output from PV at normal conditions [W]
$I_{T,sh}$	Hourly irradiance on inclined surfaces under PSC [A]
T_r	Temperature at STC [k^o]
$f_2(AOI)$	Optical effect function of AOI
$f_1(AMa)$	Air mass function
A_h	Site altitude [m]
Aj	Coefficient depending on the type of dust
ΔMj	The dust density [gm/m^2]
Z_s	Zenith angle, the angle between the vertical and the line to the sun [^{o}]

1. INTRODUCTION

The need for energy is increasing with a deficit in conventional power sources. The current trend in smart electric grids is more reliance on renewable energy sources. The photovoltaic (PV) systems are among the most important renewable energy sources due to their environmental and technical merits, which make them efficient enough to be used on large scales in both standalone and grid connected applications, with low operating and maintenance costs.

One of the most important applications of the PV systems is their standalone installations such as water pumping systems in remote areas. In sites which are isolated from the grid, it was found that installing PV water pumping systems in the site is more efficient and economic than extending the grid to reach those sites [1], [2]. Although the advantages of a standalone PV water pumping system make it a favorable option for rural agricultural areas, the deviation of its performance is unavoidable. This performance deviation is due to major ambient factors that seriously reduce the amount of the received irradiance, thus reducing the output power. These factors are partial shading condition (PSC), dust settlement on the PV array surface, air pollution, relative humidity, angle of (AOI) incidence, and air mass (AM) [3].

The presence of one or more of these factors would cause large output power fluctuations in a short time. This would lead to frequency deviation, voltage fluctuations, and flickers. These incidents will affect the quality of the power supply. This is the major drawback for the widespread introduction of PV technology into electricity grids [3]-[6].

Some recent research work has addressed the operation of PV systems under different ambient conditions. In papers [7]-[9], the influence of the temperature and the irradiance was considered in the developed mathematical model. The objective was to use those models in developing control techniques for PV islanded and grid connected operation. The partial shading condition was discussed in some recent research papers as in [9]-[15]. In those papers, it was found that the partial shading condition had the worst effect on the PV system performance, as it created multiple maximum power points, which in turn caused the malfunction of the conventional maximum power point

tracking system. Although the developed mathematical models considered the temperature and the irradiance along with the shading effect, other ambient factors were not considered.

Other research papers have expanded the modeling process to include more ambient factors as in [16]-[19]. In those papers it was found that in actual installation the PV modules operate at a wide range of angles of incidences, and air mass values. Although the modeling accuracy of the developed mathematical models has increased, the dust effect was not considered.

The dust effect was considered in some research papers such as in [20] and [21], as one of the major factors causing the reduction of the overall PV system efficiency. That reduction is due to the negative effect of the dust density decomposition on the received irradiance by PV modules. Different types of dust were studied. The developed model did not incorporate the dust effect with other factors to show their combined effect.

In this paper a novel aggregated mathematical irradiance model that incorporates all the effects of the major ambient factors is developed. An irradiance estimation method is proposed to estimate the hourly irradiance on the tilted surface of a PV array. The effect of each ambient factor is modeled on a particular component of the irradiance. The developed model is used to analyze the performance deviation of a PV system used for water pumping applications. The steps that serve this contribution are illustrated by Algorithm-1 which is implemented using MATLAB software.

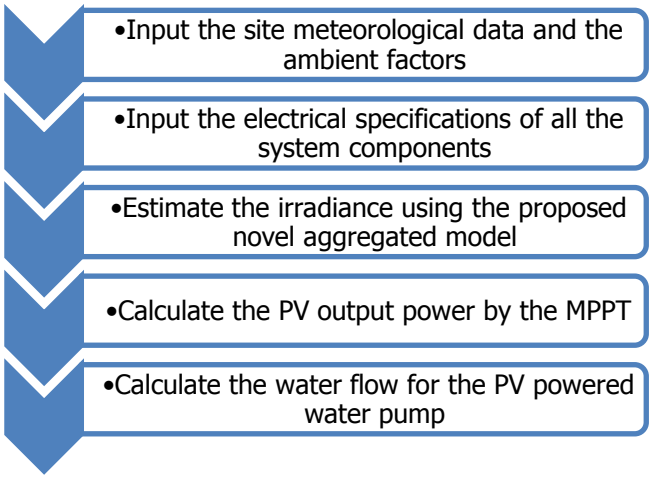

Algorithm-1: Steps of the MATLAB code for PV/Water pumping system performance analysis

This paper is organized as follows; in section 2 the novel aggregated irradiance model is proposed to include the effect of different ambient factors. An estimation model of the hourly irradiance on the tilted surface of a PV array is developed. In section 3, a case study of which the dynamic performance of a PV system connected to a DC water pumping system is investigated. Section 4 presents the main conclusions of the paper and it is followed by the references.

2. THE AGGREGATED IRRADIANCE MODEL

The hourly global irradiance on inclined surfaces $\bar{I}_T$ [w/m^2] is calculated by the following equation [22]-[24]:

$$\bar{I}_T = \bar{I}_{RT} + \bar{I}_{DT} + \bar{I}_{BT} \quad (1)$$

Each of the above mentioned ambient factors affects the PV system performance by affecting a particular component of the global hourly irradiance as explained in the following subsections.

2.1. The effect of the partial shading

The partial shading effect reduces the irradiance by the shading factor (F) which is defined as the ratio between the irradiance under shading $\bar{I}_{T,Sh}$ and the full irradiance received without shading ($\bar{I}_T$). The diffuse component is composed of the isotropic $\bar{I}_{DT,iso}$ and the circumsolar $\bar{I}_{DT,cs}$ components. The effective shading ratios are applied only to the direct component and the circumsolar part of diffuse [13]. The irradiance $\bar{I}_{T,Sh}$ received by one cell or a group of cells inside one sub-module under shading conditions is calculated from the following equation [10], [16]:

$$\bar{I}_{T,Sh} = (\bar{I}_{DT,cs} + \bar{I}_{BT})(1 - Sh) + \bar{I}_{DT,iso} + \bar{I}_{RT} \quad (2)$$

The irradiance at different shading ratios is simulated and drawn in Fig.1.

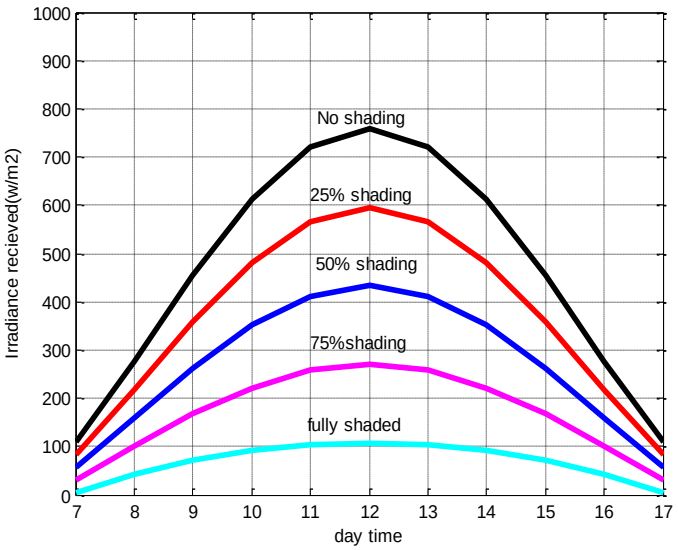

Fig.1 Irradiance $\bar{H}_{T,sh}$ (W/m^2) at different shading ratios

The extracted power from the PV module under PSC is calculated by the following equation [16]:

$$P_{Sh} = P_{NO,Sh} * \frac{\bar{I}_{T,Sh}}{\bar{I}_T} \times [1 + \tau(T - T_r)] \quad (3)$$

The integration of bypass diodes reduces the shading losses. The performance of the PV arrays with different configurations and numbers of bypass diodes is estimated according to [13].

2.2. The effect of the angle of incidence (AOI)

The angle between the incident beam on the array and the normal to that array is called the angle of incidence (AOI). The AOI influences the received irradiance by "*the optical effect*"

which accounts for the reflectivity losses. This effect is described by an empirically determined function $f_2(AOI)$. The received irradiance by the PV module under AOI effect is calculated by the following equation [16], [17]:

$$\bar{I}_T(AOI) = [f_2(AOI) \times \bar{I}_{BT}] + f_d \times \bar{I}_{DT} \quad (4)$$

Where fd is the fraction of the diffuse irradiance which is typically assumed to be 1.

A fifth-order regression is used to determine the coefficients associated with $f_2(AOI)$ as given by the following equation [14]:

$$f_2(AOI) = b_0 + b_1 + AOI + b_2(AOI)^2 + b_3(AOI)^3 + b_4(AOI)^4 + b_5(AOI)^5 \quad (5)$$

Where $b_0, b_1, b_2, b_3, b_4, b_5$ are constants.

The optical AOI effect becomes noticeable for the values larger than 60°. For the day and the site under study when considering the AOI effect, the received irradiance by the horizontal and the inclined surfaces at the daily optimum tilt angle is simulated and results are show in Fig.2 (a) and (b). The results are compared to that received irradiance without the AOI effect.

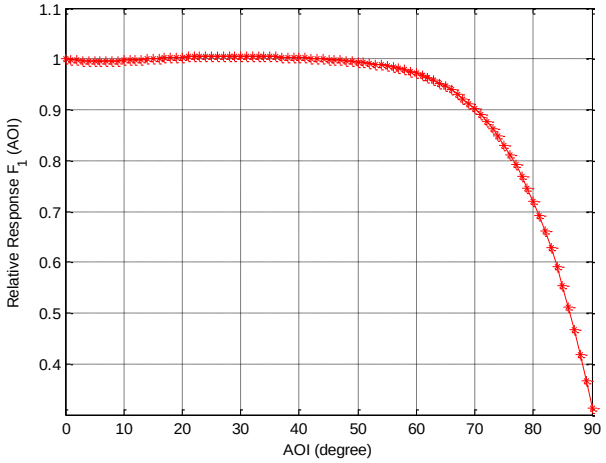

(a) Horizontal surface

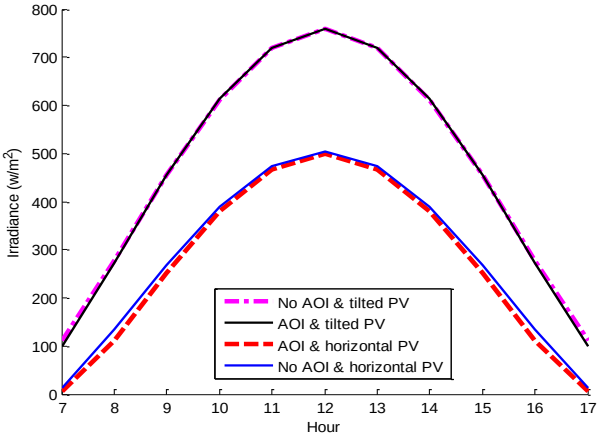

(b) Inclined surface

Fig.2 Irradiance $\bar{I}_T(AOI)$ and without AOI $\bar{I}_T$ (W/m^2)

The AOI effect is not obvious for the inclined surface because the AOI resulted was less than 60°, so this effect is obvious larger for the horizontal surface.

2.3. The effect of air mass

Air mass (AM) is the term used to describe the relative path length that the rays of the sun have to travel through the atmosphere before reaching the ground. Unity air mass condition occurs at noon. Air mass values of 10 or greater occur near sunrise and sunset. The AM effect is empirically related to the absolute air mass (AMa), resulting in the "AMa Function"$f1(AMa)$.

The air mass function depends on the type of the PV module [18], [19]. The irradiance received by the PV module with air mass effect can is calculated by the following equation [18]:

$$\bar{I}_T(AM) = \bar{I}_T \times f_1(AMa) \quad (6)$$

A fourth-order regression is used to determine the air mass function $f_1(AM_a)$ by the following equation [19]:

$$f_1(AM_a) = a_0 + a_1 \cdot AM_a + a_2(AM_a)^2 + a_3(AM_a)^3 + a_4(AM_a)^4 \quad (7)$$

Where $a_0, a_1, a_2, a_3, a_4, a_5$ are constants based on the PV type.

The absolute air mass AMa is calculated by an exponential relationship using the air mass AM and the site altitude A_h (m) by the following equation [18]:

$$AMa = AM\, e^{(-0.0001184\, A_h)} \quad (8)$$

$$AM = [(\cos(Z_s) + 0.5057 \cdot (96.080 - Z_s)^{-1.634}]^{-1} \quad (9)$$

The AM effect for different types of modules namely poly-crystalline (pi), mono-crystalline, and amorphous crystalline (ai) along day hours are shown in Fig.3.

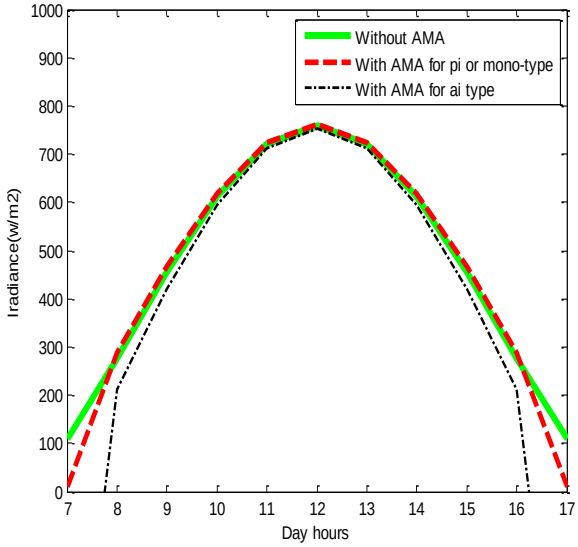

Fig.3 Irradiance at inclined surface with and without Ama

The results show that the material of the PV module is afftecting the amount of reduction in the received irrdiance when AM effect is considered.

2.4. *The effect of the dust type*

In this section, the effect of different types of dust (i.e. red soil, limestone and flying ash) on the received irradiance is studied. Since the maximum power (P_{Max}) extracted from the PV system is directly proportional to the solar irradiance, the received irradiance under the dust effect is calculated by the following equation [21]:

$$\bar{I}_T(\text{Dust}_j) = \bar{I}_T(\text{Clean}).\, e^{-Aj\Delta Mj} \quad (10)$$

When using dust density of 0.63 gm/m^2 for different dust types on the surface of BPSX150W PV module, the received irradiance is simulated as shown in Fig.4.

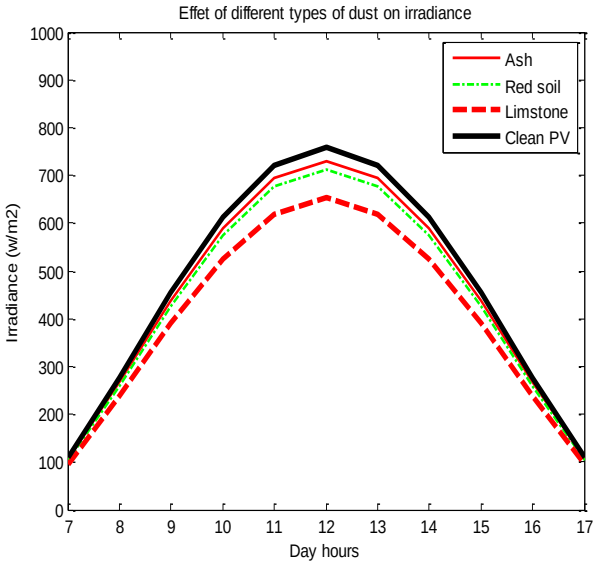

Fig.4 Irradiance received by clean surface ($\bar{I}_T$) and dusty surface ($\bar{I}_T(\text{Dust}_j)$) in (W/m^2)

From the results shown in Fig.4, it is concluded that the limestone case causes the most irradiance reduction, and then comes the red soil, and the least irradiance reduction is caused by ash.

2.5. *The Aggregated model for estimating the received irradiance under all major affecting factors*

The received irradiance by a PV module shows considerable deviation under different ambient factors discussed previously. It is essential to combine those factors in an aggregated model that accurately describes the received irradiance. The following equations show the derivation steps of the model:

1- Insert the shading effect:

$$\bar{I}_T(\text{sh}) = (1 - \text{sh})(\bar{I}_{BT} + \bar{I}_{DT,cir}) + \bar{I}_{DT,iso} + \bar{I}_{RT} \quad (11)$$

2- Add the AOI effect to Eq. (11):

$$\bar{I}_T(\text{sh}, \text{AOI}) = (1 - \text{sh})(\bar{I}_{BT} \times f_2(\text{AOI}) + \bar{I}_{DT,cir}) + \bar{I}_{DT,iso} + \bar{I}_{RT} \quad (12)$$

3- Add the AM effect to Eq. (12):

$$\bar{I}_T(\text{sh}, \text{AOI}, \text{AM}) = f_1(\text{AMa})[(1 - \text{sh})(\bar{I}_{BT} \times f_2(\text{AOI}) + \bar{I}_{DT,cir}) + \bar{I}_{DT,iso} + \bar{I}_{RT}] \quad (13)$$

4- Add the dust effect to Eq. (13):

$$\bar{I}_T(\text{All}) = [\bar{I}_T(\text{sh}, \text{AOI}, \text{AMA})]\, .e^{-Aj\Delta Mj} \quad (14)$$

The aggregated model is represented by Eq. (14). It is used to simulate the received irradiance by a PV module inclined at the optimum daily tilt angle for the day and the site under study.

In a proposed scenario, it is considered that one cell in the PV module under study is shaded by 25 % and protected by two bypass diodes, with a dust density of 0.63 gm/m^2 of ash dust, and considering both AM and AOI effects.

The received irradiance considering each of the ambient factors separately with other factors deactivated, and then with all ambient factors present is shown in Fig.5.

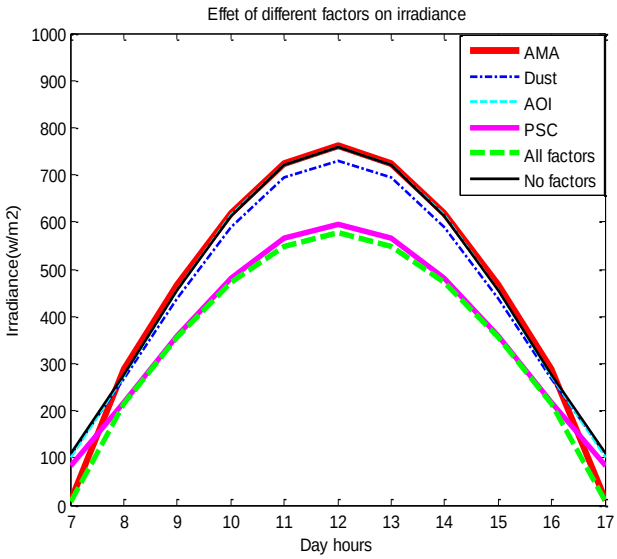

Fig.5 Irradiance received with separate effect of each ambient factor and with the combined effect of all factors in (W/m^2)

Taking the ambient factors effect into consideration shows a serious decrease in the value of the received irradiance; hence the produced PV power considerably decreased. Therefore, the study of PV system operation for different applications should look carefully at what ambient factors are present in each site under study.

Accurate estimation of irradiance leads to accurate analysis of the overall PV system performance. In the next section the PV water pumping system performance is analyzed under different ambient factors.

3. DEVELOPMENT OF PV WATER PUMPING SYSTEM

The photovoltaic water pumping system (PVWPS) consists of the PV array, the MPPT system and the motor-pump set as shown in Fig.6. The components are integrated to analyze the performance deviation under major ambient factors.

3.1. The PV Module

The PV module is modeled according to the improved PV model in [9] and PV module of type BPSX 150W [25] is used in this study.

3.2. MPPT system

The MPPT system is essential for the optimum performance of the PV system under different irradiance values, and it has to be modified to cope with multi peaks of power caused by the PSC. The MPPT system is divided into three main parts [9]:

1. DC-DC converter (the hardware): Cuk converter is selected since it is capable of achieving the optimal operation under changing irradiance and temperature values regardless of the load value [26].
2. MPPT algorithm (the software): the improved P&O tracking algorithm described in [9] is implemented to solve the drawbacks of the classic P&O.
3. MPPT Controller: the proportional integral (PI) control method is considered [27] to be capable of implementing the proposed P&O algorithm.

3.3. The motor – pump (M-P) set:

The motor pump set is selected and modeled as follows:

1. The motor:
   The Brushed DC motor is usually preferred for the PV applications [28]. The DC motor can be directly coupled with PV module or through DC-DC converter. DC motors do not need inverters which add complexity, costs and nonlinearity to the system as AC motors. DC motors are simple and cheaper than other brushless types.

2. Water pump:
   The displacement pump (DP) type is used because of its high efficiency for large range of total head. A general mathematical model links directly the operating electrical power to the water flow rate of the DP versus the total head as shown in the following equation [29]:

$$P(Q,h) = a(h)Q^3 + b(h)Q^2 + c(h)Q + d(h) \quad (15)$$

Where,

Q: The flow rate (m3/h).
h: The total dynamic head (meters).
$a(h) = a_0 + a_1h^1 + a_2\,h^2 + a_3h^3$
$b(h) = b_0 + b_1h^1 + b_2\,h^2 + b_3h^3$
$c(h) = c_0 + c_1h^1 + c_2\,h^2 + c_3h^3$
$d(h) = d_0 + d_1h^1 + d_2\,h^2 + d_3h^3$

a_i, b_i, c_i and d_i are parameters of the model and depend only on the pumping subsystem type [29].

The water pump of the type Kyocera SD 12-30 is considered because of its suitable size for the PV system under study. The rated maximum power consumption of DP under study is 150W. It operates with a low voltage (12~30V DC), and its power requirement is as little as 35W. The flow rates are up to 17.0L/min (4.5GPM) and the heads are up to 30 m (100ft) [30].

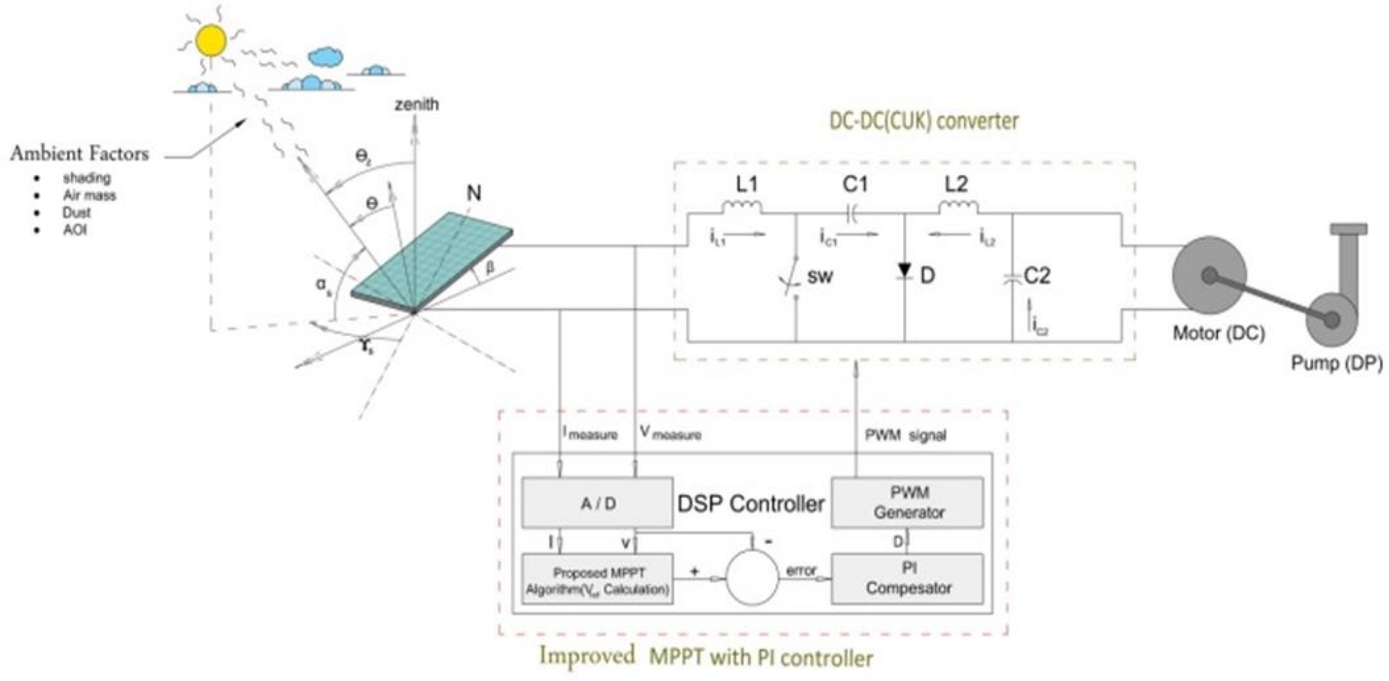

Fig.6 the of photovoltaic water pumping system

In the following section, the DC motor-pump load is connected to the PV system with the MPPT system subject to the above mentioned ambient factors.

3.4. Performance deviation analysis of the PV water pumping system: results and discussion

For the site and the day under study, the PV system is connected to the DP coupled with the DC motor through DC-DC converter. When irradiance varies along the hours of the day, the MPPT system adjusts the duty cycle to track the MPP along the hours of the day according to the improved P&O algorithm [9]. The flow rate of the pump varies with the speed of the motor which varies with the input voltage to the motor.

The performance deviation of the PV water pumping system under different ambient factors is simulated through implementing the aggregated irradiance model. A MATLAB model is developed to simulate the influence of the flow rate of DP at total dynamic head of 15m with different ambient factors.

a) The PSC effect

One cell is considered shaded artificially by any subject all the day hours with different shading ratios, with one or two bypass diodes connected to each module for the same shading ratio. The flow rate along the hours of the day for this scenario is shown in Fig.7.

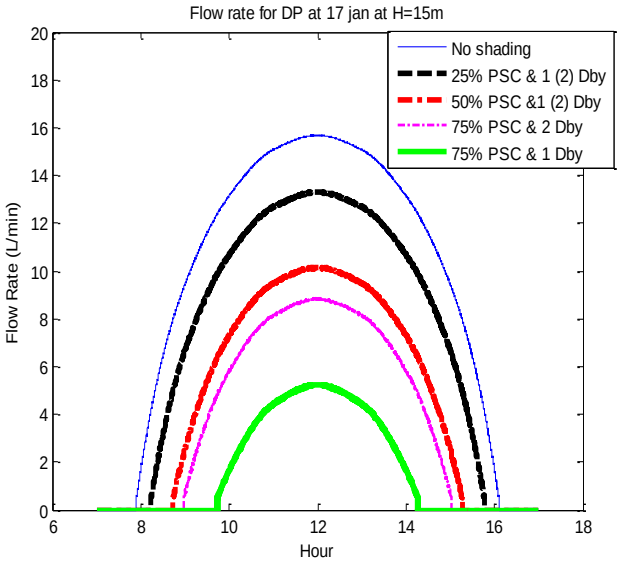

Fig.7 Flow rate with shading from DP at H=15m

From the results shown in Fig.7, the flow rate at the shading ratios of 25 % , 50% , 75% of one cell with one bypass diode is 4.1916 m^3/day , 2.3214 m^3/day and 0.0988 m^3/day respectively. The reduction in flow rate is 26.3999 %, 59.2386 %, and 98.2652 % respectively. In case of 75% PSC, when connecting 2 bypass diodes the flow rate becomes 1.5736 m^3/day, with a reduction in the flow rate of 72.3692%. From the results it is noted that for shading ratios up to 50%, the flow rate is the same for 1 and 2 bypass diodes. At higher shading ratios 2 bypass diodes increase the flow rate with about 23% than one bypass diode.

b) The AOI effect

The PV module is set on a horizontal surface and an inclined surface with the optimum daily tilt angle. For the inclined surface, the AOI is found to be less than 50° C all the hours of the day so the irradiance before and after considering the AOI effect is neglected as explained before. But when considering the horizontal PV module, the AOI values were found to be larger than 50° C for some hours of the day. The results are shown Fig.8.

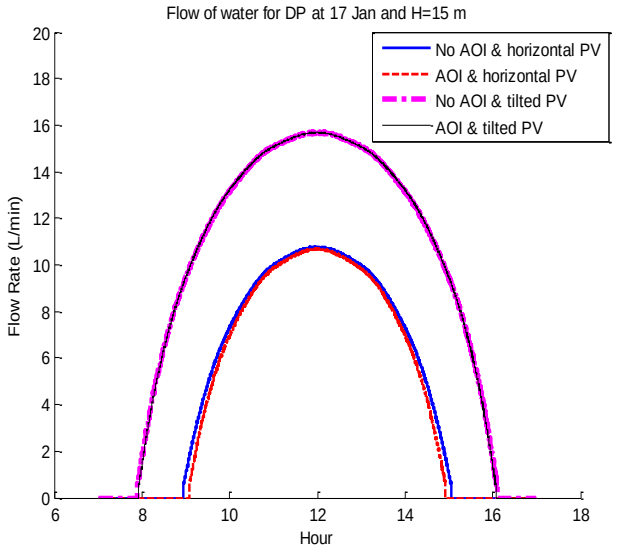

Fig.8 Flow rate with AOI effect for horizontal and inclined surface

From the results, it is noted that the flow rate is reduced from 2.8822 m3/day to 2.7502 m3/day after considering the effect of AOI. The reduction percentage in the total water flow rate is 4.6%.

c) The AM effect

The air mass effect depends mainly on the PV module type. Therefore, the water flow rate with the air mass effect is simulated for different types of amorphous (ai) and poly (pi) crystalline PV types. The results are shown in Fig.9.

From the results shown in Fig.9, the daily total volume of water is 5.6951m^3/day before considering the air mass effect for both types. After considering the air mass effect for (ai) type, it becomes 5.3072 m^3/day, with a 6.8 % reduction in the water flow. On the contrary, after considering the air mass effect for (pi) type, the water flow becomes 5.8269 m^3/day, with a 2.3% increase. This means that pi type is preferred to be used in the site under study.

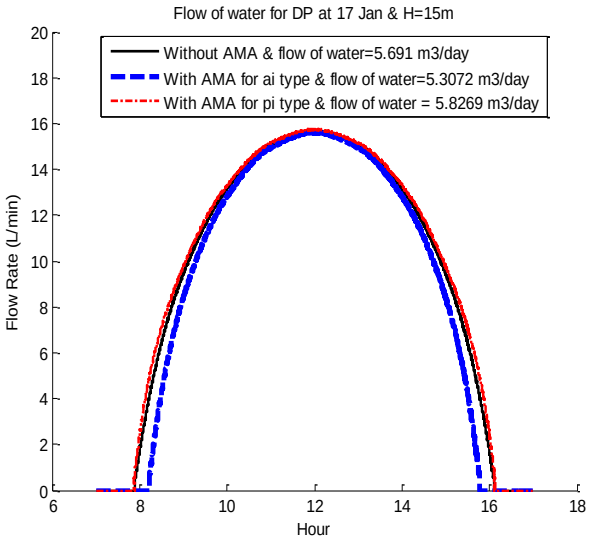

Fig. 9 Flow rate with AM effect for different PV types

d) The dust effect

Different types of dust are tested to show their effect on the water flow rate. A 0.63 gm/m^2 of ash, limestone and red soil are deposited on the PV module for the day and the site under study. The results are shown in Fig .10.

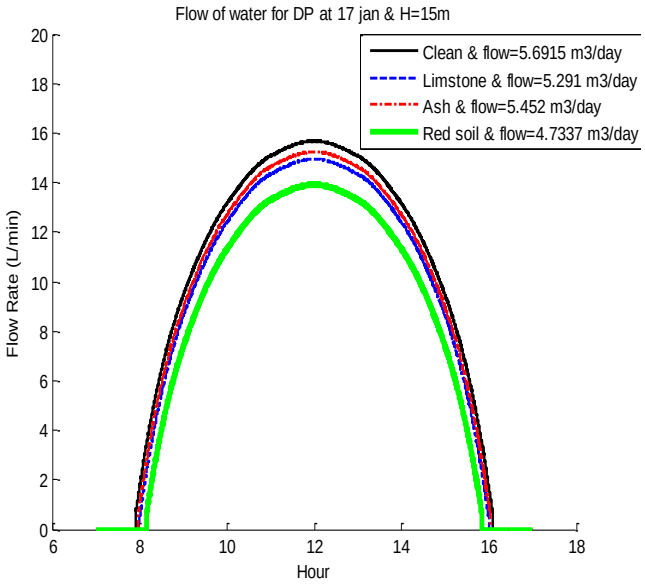

Fig.10 Flow rate with 0.63 gm/m^2 different types of dust

From the results shown in Fig.10, it is noted that the daily total volume of water flow is 5.695m^3/day under clean conditions (without the dust effect). After considering 0.63 gm/m^2 of ash, limestone and red soil, the daily total volumes of water flow are 5.452 m^3/day, 5.291m^3/day, and 4.7337 m^3/day respectively. The reduction in water flow is 4.27%, 7.09 % and 16.88% for ash, limestone and red soil respectively. This shows that the red soil has the most harmful effect on the flow

e) The effect of all the ambient factors

In the scenario of the selected day and site, where:

- One cell in the PV module which is inclined at optimum daily tilt angle is under PSC with shading ratio of 25 % due to passing clouds at hours (11, 13, 15, 16, and 17). If shaded artificially, the cell is subjected to shading for all the hours of the day.
- There are two bypass diodes over the PV module.
- Dust of red soil of 0.63 gm /m^2 is deposited.
- AM and AOI effects are considered with the PV module inclined at the optimal tilt angle and at a temperature of 50° C.
- A total dynamic head of 15 m.

In this operational scenario, each of the ambient factors is considered separately while other factors are deactivated, then all the ambient factors are considered together at artificial and clouds shading which present case A and B respectively. Then case B is repeated at T=50°C which represents case C.

By applying the proposed aggregated irradiance model, the flow rate for this scenario is shown in Fig.11. The results of the simulation are further shown recorded in Table.1.

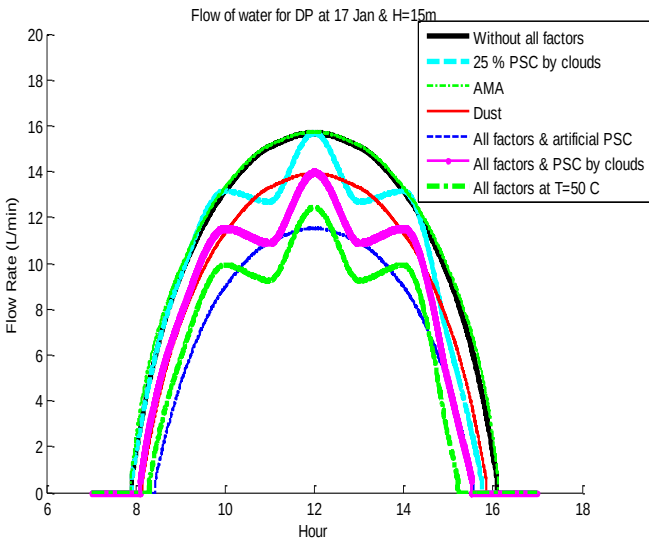

Fig.11 Flow rate considering different ambient factors

Table.1 Flow rate after considering different ambient factors

Ambient Factors	**Daily water flow (m^3/day)**
Without all factors	5.6951
25% shading by clouds	5.0505
25% artificial shading	4.1916
Effect of air mass	5.8269
Effect of 0.63 gm/m^2 red soil	4.7337
All factors with artificial PSC (caseA)	3.3773
All factors with clouds PSC (case B)	4.2363
case B at T=50°C (case C)	3.4669

From the results, the reduction in the water flow due to 25% shading by clouds of one cell with two bypass diodes is 26.4 %.

When considering the inclined PV array, the effect of the AOI is neglected, but when setting the PV array on a horizontal surface, the AOI effect reduces the daily water flow by 4.6 %.

In the same way from the simulation results, it is found that the increase in the daily water flow due to the air mass effect is equal to 2.3% for the PV type under study. It is found that the dust deposition of 0.63 g/m^2 of red soil cause a reduction in the daily water flow of 16.88%.

When combining the effect of all the ambient factors with artificial and clouds shading, the reduction in the daily flow is 40.69% and 25.6% respectively. For all the ambient factors with clouds shading at T=50°C, the reduction in the daily water flow is 39.13%.

4. CONCLUSIONS

In this paper, a novel aggregated model for estimating the irradiance values reaching the PV array under different ambient factors is proposed. The proposed model is used for the analysis of the performance deviation of a PV water pumping system. It is concluded that the consideration of the ambient factors affects the system performance largely. Therefore, there is a great need for accurate estimation of the received irradiance and hence the produced power of the PV system considering all the ambient factors for the worst and the best case scenarios. That is essential to avoid any mismatch in the sizing of the other parts of either the PV water pumping system or any other PV system application.

REFERENCES

[1] A. Mohammedi, N. Mezzai, D. Rekioua, "Impact of shadow on the performances of a domestic photovoltaic pumping system incorporating an MPPT control: A case study in Bejaia, North Algeria", Energy Conversion and Management, 2014, 84, pp. 20 -29.

[2] P. Caton, "Design of rural photovoltaic water pumping systems and the potential of manual array tracking for a west Africa village" ,Solar Energy,2014,103,pp. 288-302.

[3] D. Masa-Bote, M. Castillo-Cagigal, "Improving photovoltaic grid integration through short time forecasting and self-consumption", Applied Energy, 2014, 125, pp.103-113.

[4] J. Wong, Y.S. Lim, "Grid-connected photovoltaic system in Malaysia: A review on voltage issues", Renewable and Sustainable Energy Reviews, 2014, 29, pp. 535-545.

[5] M. M. Aly, M. Abdel-Akher, "Assessment of reactive power contribution of photovoltaic energy systems on voltage profile and stability of distribution systems", International Journal of Electrical Power & Energy Systems, 2014, 61, pp. 65-672.

[6] J. Zheng, X. Wang, Y. Chai, "The dynamic characteristics of photovoltaic generation system under partially shaded conditions", IEEE Power and Energy Engineering Conference (APPEEC), PES Asia-Pacific, 2013.

[7] M. M. El-Saadawi, A. E. Hassan, K. M. Abo-Al-Ez, M. S. Kandil, "A proposed framework for dynamic modelling of photovoltaic systems for DG applications", Taylor & Francis, 2011, 32-1, pp. 3-17.

[8] H. Altas, A.M. Sharaf, "A photovoltaic array simulation model for Matlab-Simulink GUI environment", IEEE International Conference on Clean Electrical Power (ICCEP '07), 2007.

[9] S. S. Kaddah, K. M. Abo-Al-Ez, EL-H. Abd-Raboh, S. A. Diab, "Improved MPPT algorithm using a modified PV model", 17th International Middle East Power System Conference (MEPCON'15), Mansoura University, Egypt, December 15-17, 2015.

[10] F. Martinez-Moreno, J. Muñoz, E. Lorenzo, "Experimental model to estimate shading losses on PV arrays", Solar Energy Materials and Solar Cells, 94-12, 2010, pp. 2298–2303.

[11] F. A. A. Syam, "Fault Detection of PV system using advanced simulation", Doctoral dissertation, Cairo University, Egypt, 2004.

[12] R. Rahmani, R. Yusof, E. T. Renani, "Analytical modeling of partially shaded photovoltaic systems", Energies, 2013, 6, pp. 128 – 144.

[13] S. S. Kaddah, EL-H. Abd-Raboh, K. M. Abo-Al-Ez, S. A. Diab, "Analysis and optimizing the performance of photovoltaic power systems under partial shading condition", Mansoura Engineering Journal, (MEJ), 40-3, Sept. 2015.

[14] G. Liu, P. Wang, W. Wang, "MPPT algorithm under partial shading conditions", Electrical, Information Engineering and Mechatronics, Lecture Notes in Electrical Engineering, Springer, London, 138, 2011, pp. 91 -98.

[15] D. Y. Jung , C. Y. Won , B. K. Lee, "Maximum power point tracking method for PV array under partially shaded condition" , Energy Conversion Congress and Exposition (ECCE) ,2009 , pp. 307 – 312.

[16] A. P. Dobos, "PVWatts version 1 technical reference", National Renewable Energy Laboratory (NREL) at www.nrel.gov/publications , 2013.

[17] S. V. Janakraman , J. Kuitche ,G. Tamizhni , "Validation of draft international electro technical commission IEC 61853-2 standard: angle of incidence effect on photovoltaic modules", Proc. SPIE 9179, Reliability of Photovoltaic Cells, Modules, Components, and Systems VII, 2013 ,pp. 1-44.

[18] B. Marion, "Preliminary investigation of methods for correcting for variations in solar spectrum under clear skies", National Renewable Energy Laboratory (NREL) at www.nrel.gov/publications , 2010.

[19] D. Riley, C. Hansen, "Performance model for Semprius module RDD-MOD-296, PSEL 2941", http://energy.sandia.gov/wpcontent/gallery/uploads/Semprius_perf_model_final.pdf , 2013.

[20] J. Z. Casanova, M. Piliougine, M. S. Cardona, “Analysis of dust losses in photovoltaic modules”, World Renewable Energy Congress, 2011, pp. 2985-2992.
[21] Z. Ahmed, H. A. Kazem, K. Sopian, “Effect of dust on photovoltaic performance: review and research status”, International Journal of Energy and Environment, 2013, 7-4, pp. 193- 199.
[22] J. A. Duffie, W. A. Beckman, “Solar Engineering of Thermal Processes”, John Wiley & Sons, Inc., 2013.
[23] R. Araneo, U. Grasselli, S. Celozzi, “Assessment of a practical model to estimate the cell temperature of a photovoltaic module”, International Journal of Energy and Environmental Engineering, 2014, 5-2, pp. 1-15.
[24] A. A. Trabeaa, M.A. Shaltout, “Correlation of global solar radiation with meteorological parameters over Egypt”, Renewable Energy, 2000, 21, pp. 297-308.
[25] BP SX 150 Watt Multi crystalline photovoltaic module data sheet.
[26] M. A. Farahat, H. M. B. Metwally, A. A. Mohamed, “Optimal choice and design of different topologies of DC–DC converter used in PV systems, at different climatic conditions in Egypt”, Renewable Energy, 2012, 43, pp. 393–402.
[27] S. Mekhilef , A. Patrick Hu ,N. R. Watson , “A novel MPPT algorithm for load protection based on output sensing control “ , Power Electronics and Drive Systems (PEDS), IEEE 9th International Conference ,2011, pp. 1120 – 1124 .
[28] N. Mohan, T. M. Undeland, W. P. Robbins, “Power Electronics – Converters, Applications, and Design “, 3rd Edition, John Wiley & Sons Ltd, 2003.
[29] Y. Bakellia, A. H. Arabb, B. Azouic , “Optimal sizing of photovoltaic pumping system with water tank storage using LPSP concept “ , Solar Energy , 2011 , 85-2 , pp. 288–294.
[30] Kyocera Solar Inc. Solar Water Pump Applications Guide 2001 at www.kyocerasolar.com